Published in final edited form as:
J Immunol. 2011 December 15; 187(12): 6539–6549. doi:10.4049/jimmunol.1100620.

Blocking Interleukin-1 Signaling Rescues Cognition, Attenuates Tau Pathology, and Restores Neuronal β-Catenin Pathway Function in an Alzheimer's Disease Model

Masashi Kitazawa[*,†], **David Cheng**[*,†], **Michelle Tsukamoto**[*,†], **Maya Koike**[*,†], **Paul D. Wes**[§,¶], **Vitaly Vasilevko**[*], **David H. Cribbs**[*,‡], and **Frank M. LaFerla**[*,†]

[*]Institute for Memory Impairments and Neurological Disorders, University of California, Irvine, Irvine, CA 92697-4545

[†]Department of Neurobiology and Behavior, University of California, Irvine, Irvine, CA 92697-4545

[‡]Department of Neurology, University of California, Irvine, Irvine, CA 92697-4545

[§]Roche Pharmaceuticals, Palo Alto, CA 94304

Abstract

Inflammation is a key pathological hallmark of Alzheimer's disease (AD), though its impact on disease progression and neurodegeneration remains an area of active investigation. Among numerous inflammatory cytokines associated with AD, interleukin-1β (IL-1β) in particular has been implicated in playing a pathogenic role. Here we sought to investigate whether inhibition of IL-1β signaling provides disease-modifying benefits in an AD mouse model, and if so, by what molecular mechanisms. We report that chronic dosing of 3xTg-AD mice with an IL-1 receptor (IL-1R) blocking antibody significantly alters brain inflammatory responses, alleviates cognitive deficits, markedly attenuates tau pathology, and partly reduces certain fibrillar and oligomeric forms of amyloid-β (Aβ). Alterations in inflammatory responses correspond to reduced NF-κB activity. Furthermore, inhibition of IL-1 signaling reduces the activity of several tau kinases in the brain, including cdk5/p25, GSK-3β and p38-MAPK, and also reduces phospho-tau levels. We also detected a reduction in the astrocyte-derived cytokine, S100B, and in the extent of neuronal Wnt/β-catenin signaling in 3xTg-AD brains, and provided *in vitro* evidence that these changes may, in part, provide a mechanistic link between IL-1 signaling and GSK-3β activation. Taken together, our results suggest that the IL-1 signaling cascade may be involved in one of the key disease mechanisms for AD.

Introduction

Neuroinflammation has been implicated in contributing to the etiology of Alzheimer's disease (AD), as well as in providing protective mechanisms (1-3). Whether attenuation of

Corresponding Authors: Frank M. LaFerla, Ph.D., Institute for Memory Impairments and Neurological Disorders, Department of Neurobiology and Behavior, University of California, Irvine, 3212 Biological Sciences III, Irvine, CA 92697-4545, Tel: 949-824-1232, Fax: 949-824-7356, laferla@uci.edu; Masashi Kitazawa, Ph.D., Institute for Memory Impairments and Neurological Disorders, Department of Neurobiology and Behavior, University of California, Irvine, 3208 Biological Sciences III, Irvine, CA 92697-4545, Tel: 949-824-5902, Fax: 949-824-7356, kitazawa@uci.edu.
[¶]Current address: Neuroscience, Bristol-Myers Squibb, 5 Research Parkway, Wallingford, CT 06492

inflammatory pathways will offer therapeutic benefit for AD remains unclear. Nevertheless, epidemiological and prospective population-based studies show an association between suppression of inflammation and reduced risk for AD (4-7). Furthermore, pro-inflammatory cytokines, such as interleukin-1 (IL-1), interleukin-6 (IL-6) and tumor necrosis factor α (TNFα), are elevated in the plasma, brains, and cerebrospinal fluid of patients with AD or mild cognitive impairment (MCI), whereas anti-inflammatory cytokines are decreased (8-15). Large-scale gene array studies have also identified significant upregulation of inflammatory-related genes in the brains of AD patients compared to age-matched cognitively normal individuals (16, 17). Moreover, many of the genes that are most significantly associated with the risk of developing AD, including *clusterin (CLU), complement component receptor 1 (CR1), CD33, CD2AP*, *IL1A, IL1B, IL8*, and *TNF*, are inflammatory genes (18-24).

Based on these observations, both *in vitro* and *in vivo* studies have been conducted to elucidate the role of inflammation in the pathogenesis of AD. For example, treatment of a tauopathy mouse model with the immunosuppressant, FK506, rescued tau pathology and increased lifespan, supporting the hypothesis that inflammation contributes to disease progression (25). Similarly, inhibition of TNFα signaling has been shown to attenuate AD-like pathology and cognitive impairments in transgenic mouse models, as well as in AD patients (26-28), whereas upregulation of TNFα has been shown to exacerbate AD pathology. Another pro-inflammatory cytokine, IL-1β, also appears to play an important role in AD. IL-1β has been reported to increase the expression of APP in neuronal culture (29, 30), and exposure of primary neurons to IL-1β exacerbates tau phosphorylation through aberrant activation of p38-MAPK (31). In transgenic mouse models, IL-1β or elevated inflammatory responses in the brain increase neuronal tau phosphorylation and tangle formation (25, 32, 33). In contrast, a recent study found that overexpression of IL-1β reduces Aβ-related pathology by modulating innate immune responses or promoting non-amyloidogenic APP cleavage in a mouse model of AD and in a cell culture model, suggesting that IL-1β may play a beneficial role in limiting AD pathology (34, 35). However, the transgene construct used in the *in vivo* study by-passed the highly-regulated pathway for IL-1β release and was expressed in cells of neuronal lineage (astrocytes), rather than a physiological hematopoietic cell type, such as microglia, and therefore may not reflect the physiology role of IL-1β in disease (34). To directly test whether inhibition of IL-1β signaling has the potential for alleviating AD-relevant pathology, we treated a mouse model that exhibits both Aβ and tau pathology (3xTg-AD) with an IL-1 receptor (IL-1R) blocking antibody (anti-IL-1R), and evaluated the consequences of this treatment on pathology and molecular changes. We found that anti-IL-1R treatment regulated brain inflammatory responses through the reduction of NF-κB activity and partly reduced fibrillar and oligomeric Aβ species, albeit without reducing overall Aβ plaque burden. Notably, however, neuronal tau pathology was markedly attenuated in the anti-IL-1R-treated animals. The effect on tau correlated with reduced activation of cdk5/p25, GSK-3β and p38-MAPK. We also detected a significant reduction in the levels of S100B, an astrocyte-derived cytokine, and the extent of Wnt/β-catenin signaling in neurons. These changes may, in part, explain the mechanistic link between IL-1 signaling and GSK-3β activation. Therefore, the present study provides evidence that abrogating IL-1β signaling may offer therapeutic

benefit to AD patients, and begins to elucidate the putative underlying mechanisms of action for such a treatment.

Materials and Methods

Animals and treatment paradigm

All experiments were carried out in accordance with the Institutional Animal Care and Use Committee at the University of California, Irvine, and were consistent with Federal guidelines. 200 μg of rat anti-IL-1R blocking antibody (Roche Pharmaceuticals, Palo Alto, CA) was administered intraperitoneally to 9-month old 3xTg-AD mice (Thy1.2-APP_{swe}, Thy1.2-Tau_{P301L}, $PS1_{M146V}$-KI) every 8-9 days for 6 months. The control groups received vehicle (10 mM histidine and 150 mM NaCl, pH 6.5), whereas the isotype-matched IgG control group received 200 μg of rat IgG in the same manner. Each group consisted of an equal number of males and females, and the total number of mice was 12 per group.

Upon the completion of the treatment period, mice were anesthetized, and blood was collected from the right ventricle of heart. Then, mice were perfused with ice-cold phosphate buffered saline, and brains were collected. One hemisphere of the brains were fixed with 4% paraformaldehyde for immunostaining. The other hemispheres were first homogenized in T-PER buffer containing protease/phosphatase inhibitors followed by the centrifugation at 100,000g for 1 hr to separate the detergent-soluble fraction and insoluble pellets. Pellets were subsequently homogenized in 70% formic acid and the detergent-insoluble fractions were collected. Collected blood was briefly centrifuged to isolate plasma. Plasma samples were placed on silicated test tubes and stored at -80°C until further analysis.

For the detection of anti-IL-1R antibody in the brain, we first biotinylated and subsequently purified the anti-IL-1R blocking antibody by EZ-LINK Sulfo-NHS-LC-Biotin kit (Pierce Biotechnology, Rockford, IL) according to manufacturer's instructions. We intraperitoneally (i.p.) injected approximately 200 μg of biotinylated anti-IL-1R blocking antibody into aged 3xTg-AD mice, and brains were collected at 6 or 24 hrs after the antibody injection following the method described above. Biotinylated antibody was detected using streptavidin-HRP conjugates (for immunoblot) or by streptavidin-Alexa488 conjugates (for immunofluorescent staining) in the tissue homogenates or sliced brain sections, respectively.

Cognitive tests

Following 6 months of antibody treatment, all mice were subjected to cognitive evaluation in the Morris water maze (MWM) and contextual fear conditioning (CFC) tests (36, 37). MWM primarily measures hippocampal-dependent cognition, whereas CFC assesses both amygdala and hippocampal function, including the trisynaptic pathway (entorhinal cortex, dentate gyrus, CA3, and CA1). Briefly, the apparatus used for the Morris water maze (MWM) task was a circular aluminum tank (1.2 m diameter) painted white and filled with water maintained at 22–24 °C. The maze was located in a room containing several simple visual, extramaze cues. Mice were trained to swim and find a 14 cm diameter circular clear Plexiglas platform submerged 1.5 cm beneath the surface of the water and invisible to the mice while swimming. On each training trial, mice were placed into the tank at one of four

designated start points in a pseudorandom order. Mice were allowed to find and escape onto the platform. If mice failed to find the platform within 60 sec, they were manually guided to the platform and allowed to remain there for 10 sec. Each day, mice received 4 training sessions separated by intervals of 25 sec under a warming lamp. The training period ended when all groups of mice reached criterion (<25 sec mean escape latency). The probe trial to examine retention memory was assessed 24 hours after the last training trial. In the probe trials, the platform was removed from the pool, and mice were monitored by a ceiling-mounted camera directly above the pool during the 60 sec period. All trials were recorded for subsequent analysis. The parameters measured during the probe trial included (1) latency to cross the platform location, and (2) number of platform location crosses.

Contextual fear conditioning (CRC) test was performed using the Gemini Avoidance System (San Diego Instruments, San Diego, CA) (37). The training trial consisted of placing a mouse in the illuminated compartment of the device, and recording the time required for it to enter the dark compartment (baseline latency). Upon entering, the door between the two compartments was closed and the mouse immediately received an electric shock to the feet (0.15 mA, 1 sec). During the retention trial (conducted 24 hours after the training trial), the mouse was again placed in the illuminated compartment and the latency to enter the dark compartment was recorded. The retention trial was interrupted if the animal took more than 180 sec to cross into the dark compartment.

Antibody titer

The titers of mouse anti-rat immunoglobulins antibodies were measured by ELISA as previously described, with minor modifications (38, 39). Briefly, 96-well plates (Immulon 2HB, Thermo Fisher Scientific, Waltham, MA) were coated with 1.0 μM of the rat anti-IL-1R monoclonal antibody used for passive injection in carbonate coating buffer (CCB) pH 9.6 (Sigma-Aldrich, St. Louis, MO) and incubated overnight at 4°C. The wells were washed and blocked with 3% non-fat dry milk for 1 hour at 37°C with shaking. After washing, serial dilutions of all plasma samples, collected at the end of 6-month treatment, were added to the wells and plates were incubated for 2 hours at 37°C with shaking. After washing, HRP-conjugated affinity purified donkey anti-mouse IgG antibodies with minimal cross-reactivity with other species (Jackson ImmunoResearch Laboratories, West Grove, PA) were added at 1:2000 dilution for 1 hour at 37°C with shaking, wells were washed, and Ultra-TMB ELISA substrate (Pierce Biotechnology) was added for 15 min to develop the reaction. The reaction was stopped by adding 2 N H_2SO_4 and plates were analyzed on a Synergy HT Spectrophotometer (Bio-Tek Instruments, Winooski, VT) at 450 nm. The plasma end-point titer was defined as the maximal plasma dilution in which the OD for the antibodies was 3 times higher than the OD values of the blank wells.

Primary astrocyte culture

Primary astrocytes were isolated from postnatal day 1 (P1) C57BL/6 mice. Briefly, brains were dissected, minced and trypsinized for 20 min at 37°C. Tissues were then triturated, and grown in DMEM/F12 supplemented with 10% FBS and penicillin and streptomycin for 6 days. When cells were confluent, astrocytes were purified by shaking at 350 rpm for 24 hrs at 37°C. Attached cells were trypsinized and cultured on slide chambers to evaluate the

purity of astrocytes by staining with GFAP (astrocyte marker), Iba1 (microglia marker), CNPase (oligodendrocyte marker), and β-tubulin (neuronal marker), or on 6-well plates for treatments.

Primary astrocytes were exposed to 0.5-3 ng/ml mouse recombinant IL-1β (Sigma-Aldrich) for 24 hrs. Conditioned media were collected for treatments of SH-SY5Y cells, and astrocytes were homogenized with M-PER reagent containing protease and phosphatase inhibitors to collect proteins. Extracted proteins were used for Western blotting to measure S100B.

Cell culture studies

Human neuroblastoma SH-SY5Y cells were grown in DMEM/F12 supplemented with 10% FBS and penicillin and streptomycin. Cells were exposed to conditioned media collected from primary astrocytes for 24 hrs, and cytosolic and nuclear proteins were extracted as follows. Cytosolic fractions were collected by lysing cells with buffer containing 10 mM HEPES, pH 7.9, 1.5 mM $MgCl_2$, 10 mM KCl, 0.5 M DTT, 0.05% NP40, and protease and phosphatase inhibitors. Cells were centrifuged at 3000 rpm for 10 min at 4°C, and supernatant was used as cytosolic fraction. Pellets were re-suspended with buffer containing 5 mM HEPES, pH 7.9, 1.5 mM $MgCl_2$, 0.2 mM EDTA, 0.5 mM DTT, 0.3 M NaCl, 26% glycerol (v/v) and protease and phosphatase inhibitors. After homogenizing pellets, the suspension was left on ice for 30 min, centrifuged at 24,000g for 20 min at 4°C. Supernatant was used as nuclear fraction.

For treatment with S100B protein, SH-SY5Y cells were plated on 6-well culture plates, and S100B from bovine brain (Sigma-Aldrich) was added to a final concentration of 0.05-5 μM. After 24 hrs of incubation, cells were homogenized with M-PER (Pierce Biotechnology) supplemented with protease and phosphatase inhibitors and centrifuged to collect total lysates for immunoblot analysis. All *in vitro* experiments were performed and analyzed in 2-3 independent experiments in triplicates or quadruplets.

Cytokine assays

Brain or plasma cytokines were quantitatively measured by ELISA (Pierce Biotechnology) or Bio-Plex (Bio-Rad Laboratories, Hercules, CA), respectively, as described previously (40). Briefly, 50 μl of brain homogenates were used to determine IL-1β, IL-6 and TNFα levels by Endogen ELISA kits. For Bio-Plex, we used a custom 8-plex detection kit, which measured IL-1α, IL-1β, IL-4, IL-6, IL-10, monocyte chemoattractant protein-1 (MCP-1), TNFα, and interferon-γ (IFNγ). We strictly followed the manufacturer's instructions. Briefly, 10 μl of plasma was mixed with 40 μl of standard diluent and incubated with a mixture of antibodies conjugated with fluorescent beads. Following the detection antibody and streptavidin-PE treatments, levels of each cytokine were measured using the Bio-Plex 200 System (Bio-Rad Laboratories). Concentrations were calculated by standard curve and expressed in pg/ml.

Western blot analysis

Protein concentrations of detergent-soluble fractions from half brain (cortex and hippocampus) were determined by the Bradford protein assay. These fractions were subsequently immunoblotted with the following antibodies: HT7 (total human tau, Pierce Biotechnology), AT8 (phosphorylated tau at S199/S202/T205, Pierce Biotechnology (41)), PHF-1 (phosphorylated tau at S396/S404, Pierce Biotechnology), AT100 (phosphorylated tau at S212/T214, Pierce Biotechnology), total p65 NF-κB (Cell Signaling Technology, Beverly, MA), phospho-p65 NF-κB (phosphorylation at S536, Cell Signaling Technology), YM1 (Stem Cell Technologies, Vancouver, Canada), arginase-1 (Santa Cruz Biotechnology, Santa Cruz, CA), cdk5 (Calbiochem, La Jolla, CA), p35/p25 (Santa Cruz Biotechnology), GSK-3β (BD transduction laboratories, San Jose, CA), phospho-GSK-3β (phosphorylation at S9), p38-MAPK, phospho-p38-MAPK (phosphorylation at T180/Y182), Akt, phospho-Akt (phosphorylation at S473, all from Cell Signaling Technology), S100B (Novus Biologicals, Littleton, CO), β-catenin (Sigma-Aldrich), and phospho-β-catenin (phosphorylation at S552 or S31/S37/T41, Cell Signaling Technology). Membranes were re-probed with antibody against β-actin (Sigma-Aldrich), GAPDH (Santa Cruz Biotechnology) and/or nuclear matrix p84 (Abcam, Cambridge, MA) to control for protein loading or to confirm no cross-contamination of each fraction. Band intensity was measured using Quantity One software (BioRad Laboratories) and normalized by corresponding loading control proteins.

Dot blot analysis was used to quantitatively measure oligomeric species of Aβ. Conformation specific anti-oligomer antibodies, A11 and OC, were used (kind gift from Dr. C. Glabe, UC Irvine). Briefly, 3 μg of brain homogenates were spotted on nitrocellulose membrane. After blocking non-specific binding, A11 or OC antibody was applied, and membrane was incubated overnight at 4°C. Subsequently, secondary anti-rabbit HRP-conjugated antibody was used to detect A11 or OC antibody.

Immunohistochemical analysis

For immunohistochemical analysis, each half brain was cut into 50 μm slices using a Vibratome and stored in TBS. To qualitatively assess Aβ plaque burden, free-floating sections were pre-treated with 90% formic acid for 7 min and incubated with biotinylated antibody against $A\beta_{42}$ (clone D32 from Drs. Vasilevko and Cribbs, 1:400) overnight, followed by ABC reagent for 1 hour. Sections were washed with TBS and visualized by DAB according to the manufacturer's specifications. IL-1 receptor expression in the brain was visualized by staining with IL-1R blocking antibody (1:100) followed by incubation with biotinylated anti-rat secondary antibody (Vector Laboratories, Burlingame, CA, 1:200) and visualized with DAB. Sections were counterstained with hematoxylin to visualize nuclei. For phospho-tau qualitative analysis, sections were stained with AT8 (1:2000), AT100 (1:2000), and HT7 (1:2000) in the same manner. To assess microglial activity around Aβ plaques, free-floating sections were pretreated with 90% formic acid for 6 minutes then stained for Aβ plaques using 6E10 (1:400) and microglia with anti-Iba-1 (1:400), CD68 (1:100, Serotec, Raleigh, NC) or YM1 (1:100) overnight. To visualize co-localization, sections were incubated for 1 hour with goat anti-mouse Alexafluor 488 and goat anti-rabbit Alexfluor 555, with TOTO3 (1:200) for nuclear staining. The co-localization

of IL-1β in microglia was assessed by staining sections with anti- IL-1β (1:100) and Iba-1 (1:1000) overnight, followed by secondary antibodies donkey anti-goat 488 and donkey anti-rabbit 555.

Semi-quantitative analysis of plaque burden

Aβ plaque burden in hippocampus, subiculum, entorhinal cortex and amygdala was quantified by counting plaques (larger than 20 μm in diameter) or measuring the areas occupied by plaques. Briefly, three brain sections from each animal were stained with anti-$Aβ_{42}$ antibody described above, and images were captured using Zeiss Axioskop with Axiocam (Carl Zeiss Microimaging, Thornwood, NY). $Aβ_{42}$-positive plaques were counted in 500 $μm^2$ subfield in hippocampus, subiculum, entorhinal cortex and amygdala. Plaque burden was calculated by defining approximate areas of plaques over the entire areas in hippocampus, subiculum, entorhinal cortex and amygdala using ImageJ software.

Quantitative analysis of Aβ by ELISA

$Aβ_{40}$ and $Aβ_{42}$ were detected in both the detergent-soluble and -insoluble fractions by enzyme-linked immunosorbent assay (ELISA) as described previously (32).

Real-time PCR

Total RNA was isolated from untreated or treated SH-SY5Y cells using TRI reagent (Molecular Research Center, Cincinnati, OH). Briefly, 1 μg of total RNA was used for one-cycle reverse transcriptase reaction to make cDNA by random hexamers using SuperScript III first-strand synthesis system (Invitrogen, Carlsbad, CA). 1 μl of resulting cDNA was subjected to a PCR reaction for the detection of S100B using iQ SYBR Green supermix (Bio-Rad Laboratories). Human S100B primers were 5′- TGG ACA ATG ATG GAG ACG G-3′ (forward) and 5′- ATT AGC ACA ACA CGG CTG G-3′ (reverse) (42). GAPDH was used for normalizing the S100B expression levels in each treatment, and the primer sequences were 5′-AAC TTT GGC ATT GTG GAA GG-3′ and 5′-ACA CAT TGG GGG TAG GAA CA-3′. The PCR cycle parameters were as follows: denaturing step (95 °C for 30 sec), annealing step (60 °C for 30 sec) and extension step (72 °C for 30 sec). The cycle threshold (Ct) values were determined by MyiQ software (Bio-Rad Laboratories), and ΔCt for each treatment group was calculated as follows: ΔCt = Ct (S100B) - Ct (GAPDH). The RQ was then calculated by the following equation: $RQ = 2^{-ΔΔCt}$, with ΔΔCt = ΔCt (treatment) - ΔCt (control) (43).

Statistical analysis

All immunoblot and immunohistochemical data were quantitatively analyzed using Bio-Rad Quantity One software or Image J software. Statistics were carried out using one-way ANOVA with post-hoc tests or unpaired t-test, and $p<0.05$ was considered to be significant.

Results

Blocking IL-1 receptor reduces NF-κB activation in the brain

To suppress IL-1 signaling, we administered an IL-1R blocking antibody (anti-IL-1R) to 9-month old 3xTg-AD mice over the course of 6 months using the same paradigm as a prior study with anti-CD40 antibody in PDAPP mice (44). During the 6 months of dosing, 2 control mice, 2 IgG-treated mice and 4 anti-IL-1R-treated mice died. No clear signs of autoimmune responses or CNS damage were observed. All data presented in this study were obtained from mice that survived the entire experimental procedure. Immunohistochemical studies confirmed that astrocytes, microglia, endothelial cells of blood vessels, and, to some extent, neurons were recognized by the anti-IL-1R antibody, consistent with reported expression patterns (45) (Suppl. Fig. 1A, B).

At the end of the 6-month treatment, we measured plasma antibody titers against rat antibodies, the species in which anti-IL-1R was generated, and found that they were 0.516 ± 0.049 for untreated mice, 1.420 ± 0.354 for IgG control (sham-treated mice), and 1.354 ± 0.330 for the anti-IL-1R treated mice, with the titers reaching 1:1,600, which suggests an induction of low levels of anti-rat antibodies in both IgG- and anti-IL-1R-treated animals. We also examined whether the IL-1R blocking antibody crossed the blood-brain barrier (BBB). It has been reported in numerous studies that antibodies administered peripherally by i.p. injections cross the BBB and exhibit their effects centrally, particularly in AD research treating transgenic mouse models with antibodies against Aβ (44, 46-52). In our study, we attempted to identify anti-IL-1R antibody binding in the CNS of the treated 3xTg-AD mice using a double immunofluorescent staining, but the result was inconclusive although we did observed an increased signal for anti-IL-1R antibody on microglia, astrocytes and neurons at the end of the 6-month treatment (data not shown). We then examined the antibody penetration of the BBB at earlier time points. The anti-IL-1R antibody was first biotinylated, then injected intraperitoneally in the 3xTg-AD mice. The presence of the biotinylated antibody in the brain was measured biochemically and histochemically after 6 and 24 hrs post-injection. A 50 μg of protein extract from a half brain was loaded, and the presence of biotinylated anti-IL-1R antibody was detected by a streptavidin-HPR conjugate. A significant increase of the biotinylated anti-IL-1R antibody (shown as heavy and light chains, arrowheads) in the brain was detected in both 6- and 24-hr anti-IL-1R antibody-treated 3xTg-AD mice by immunoblot while virtually no biotinylated antibody was present in untreated control 3xTg-AD mice (Suppl. Fig. 1C). The binding of anti-IL-1R antibody in CNS cells was further confirmed by a double immunostaining (Suppl. Fig. 1D). A fraction of neurons and blood vessels in brain sections from untreated control 3xTg-AD mice were positive by streptavidin-Alexa488 (Suppl. Fig. 1D i from CA1 hippocampus and ii from cortex, arrowheads), suggesting endogenous non-specific biotinylated molecules or proteins that were also detected by western blot (Suppl. Fig. 1C). On the other hand, it was clear that the biotinylated anti-IL-1R antibody was present on the surface of microglia, astrocytes, neurons and endothelial cells in the brain sections from the biotinylated anti-IL-1R antibody-injected 3xTg-AD mice (Suppl. Fig. 1D v-x, arrows). This colocalization was minimal in the control mice (Suppl. Fig. 1D ii-iv). Together, these data suggest that a small proportion of the systemically administered anti-IL-1R antibody crossed the BBB in the

3xTg-AD mice. In addition, brain NF-κB activity, measured by the steady-state levels of phosphorylated p65 at Ser536, was significantly reduced in the anti-IL-1R-treated mice, further suggesting an antagonizing action of the antibody in CNS (Suppl. Fig. 2A). However, it is important to point out that we cannot exclude a possibility that any downstream effects described in this study might be due not only to direct action in the CNS but also to peripheral effects of blocking IL-1 receptor.

Blocking IL-1 signaling rescues AD-related cognitive impairments

The effect of IL-1 signaling on cognition was assessed by Morris water maze (MWM) and contextual fear conditioning (CFC) tests. In the acquisition phase, the IL-1R blocking antibody-treated mice reached criteria (escape latency at 20 sec) on the 4th day of the training and performed significantly better than control or sham-treated group (Fig. 1A; $p<0.05$). The control or sham-treated group reached criteria on the 5th or 6th day, respectively, and there was no overall statistical difference between these two groups. In the 24-hr probe trial to test hippocampal-dependent retention memories, we found that blocking IL-1 signaling significantly improved both escape latency and the number of platform crosses (Fig. 1B-C; $p<0.05$). Similarly, the anti-IL-1R-treated mice performed significantly better on this cognitive test versus control or sham-treated mice in the CFC test (Fig. 1D; $p<0.05$). Thus, blocking IL-1 signaling in the 3xTg-AD mice rescued hippocampal-dependent cognitive impairments as measured by two independent behavioral tests.

Aβ plaque pathology is marginally affected following suppression of IL-1 signaling

We next assessed the effects of blocking IL-1 signaling in aged 3xTg-AD mice on Aβ pathology. Quantitative Aβ ELISA revealed a significant reduction of detergent-insoluble $Aβ_{42}$, but not $Aβ_{40}$, in the brains of anti-IL-1R-treated animals (Fig. 2B; $p<0.05$). Interestingly, soluble Aβ levels were either unchanged or increased with anti-IL-1R treatment (Fig. 2A). Histological analysis revealed that the number of plaques over 20 μm diameter in hippocampus, subiculum, entorhinal cortex and amygdala was significantly reduced with anti-IL-1R treatment when compared to control group, which was in part supported the quantitative ELISA data described above (Fig. 2C, E; $p<0.05$, and Suppl. Fig. 3). On the other hand, the Aβ plaque burden failed to show any significant difference among the treatment groups, and it was in part because of the unevenly distributed plaques within the each mouse brain and variability among individual mice within the treatment group (Fig. 2C, D and Suppl. Fig. 3). Similarly, soluble proto-fibrillar and fibrillar Aβ oligomers detected by conformational specific antibodies, A11 and OC, respectively, showed mixed results. Although proto-fibrillar Aβ oligomers were unaffected, fibrillar Aβ oligomers were markedly reduced in the aged 3xTg-AD mice that received the IL-1R blocking antibody (Fig. 2F, G, and Suppl. Fig. 2B). APP expression or processing was not significantly altered by the treatment, as the steady-state levels of APP or C-terminal fragments of APP, such as C99 and C83, were not changed among the treatment groups (Fig. 2H). Collectively, these results suggest that blocking IL-1 signaling may be capable of reducing certain fibrillar or oligomeric Aβ species and has marginal effects on blocking maturation or formation of Aβ plaques.

Anti-IL-1R treatment attenuates microglial activation in 3xTg-AD brains

Despite modest changes in Aβ pathology, pro-inflammatory and microglial responses were found to be altered in the brain following anti-IL-1R treatment of aged 3xTg-AD mice. The levels of the pro-inflammatory cytokines, IL-1β and TNFα, in the brain were significantly decreased when IL-1 signaling was blocked (Fig. 3A). IL-6 showed a trend towards reduction, but did not achieve significance (Fig. 3A). However, it is important to note that the levels of these pro-inflammatory cytokines were significantly higher than age-matched non-transgenic mice even with anti-IL-1R treatment (data not shown), suggesting that the anti-IL-1R treatment did not completely suppress pro-inflammatory responses in the brain. Double immunofluorescent staining further confirmed the reduction of IL-1β production in activated microglia around plaques (Fig. 3B).

These changes in the brain milieu may affect the phagocytic abilities of microglia. Double immunofluorescent staining detected that the number of microglia harboring 6E10-positive APP/Aβ fragments was increased, suggesting that these cells were actively engulfing Aβ (control - 4.8/20 cells; sham - 6.2/20 cells; IL-1R - 12.2/20 cells, using 40x field, representative figures in Fig. 3C). Additional staining was conducted to further analyze the microglial phenotype using several markers, CD68, YM1 and arginase-1, that have been previously described as phagocytic markers (53, 54). Although CD68-positive microglia were uniformly detected around plaques in all groups (data not shown), more YM1-positive microglia were observed in the anti-IL-1R-treated mice (Fig. 3D). Quantitative analysis of YM1 and arginase-1 showed significant increases in the brain of the anti-IL-1R-treated 3xTg-AD mice. Therefore, anti-IL-1R-treatment appears to increase the phagocytic activation of microglia (Suppl. Fig. 2C). The levels of two major amyloid-degrading enzymes that are secreted from microglia, insulin-degrading enzyme (IDE) and neprilysin (NEP), were, however, not significantly altered in the brain (Fig. 3E).

Tau pathology is significantly attenuated following anti-IL-1R treatment of aged 3xTg-AD mice

We and others previously demonstrated that altered inflammation in the brain significantly influenced the subsequent development of tau pathology, independent of Aβ pathology, in the 3xTg-AD mice and other mouse models (25, 32, 53). Consequently, we next investigated pathological changes in tau following anti-IL-1R treatment of aged 3xTg-AD mice. Blocking IL-1 signaling significantly reduced the number of phospho-tau-bearing neurons detected by antibodies AT8 (pSer199/Ser202/Thr205) and AT100 (pSer212/Thr214) in the CA1 subfield of the hippocampus while no clear alteration in total tau by the antibody HT7 was detected in the same field (Fig. 4A). This change was also evident by immunoblotting, as AT8- , AT100- or PHF-1 (pSer396/Ser404)-positive phospho-tau levels were significantly reduced in mice after treatment, whereas the steady-state levels of total tau remained unchanged (Fig. 4B, Suppl. Fig. 2D).

The reduction of phospho-tau levels in the brain was accompanied by a significant reduction of p25 levels ($p<0.01$), increased levels of phospho-GSK-3β (at Ser9 position) and a reduction of phospho-p38-MAPK in the brains of the anti-IL-1R-treated mice, which are predicted to lead to lower activity of cdk5, GSK-3β and p38-MAPK, respectively (Fig. 4C).

The total steady-state levels of cdk5, GSK-3β and p38-MAPK were not significantly altered among the treatment groups (Fig. 4C). The sum of these results highlights the diverse disease-modifying effects of blocking IL-1 signaling.

IL-1 modulates S100B secretion in astrocytes and suppresses β-catenin signaling in neurons

It is not clear whether IL-1 signaling directly affected neurons and regulated intraneuronal signaling cascades, or whether the pathology was affected by other cell types in the brain or the periphery. Indeed, the role of IL-1 signaling in AD etiology may be pleitropic, and activities of the kinases identified here, p38-MAPK, cdk5 and GSK-3β, may influence multiple signaling cascades in multiple cell types. For instance, it has been demonstrated that IL-1 signaling activates p38-MAPK in neurons, leading to tau phosphorylation (31, 53, 55). At the same time, IL-1 signaling promotes production of IL-1β and other pro-inflammatory molecules by microglia, astrocytes, and peripheral inflammatory cells, in part, via a p38-MAPK cascade (56-58). Therefore, the reduction of p38-MAPK activation we observe in response to anti-IL-1R treatment may be due to the action of inhibiting IL-1 signaling in peripheral inflammatory cells, microglia and astrocytes, as well as neurons.

The relationship between IL-1 signaling and the activation of cdk5 and GSK-3β are less well characterized. Therefore, we sought to better understand the underlying mechanisms by which activities of these tau kinases were suppressed following anti-IL-1R treatment. Since IL-1β regulates the expression and secretion of a key AD-relevant cytokine, S100B, from astrocytes (59-61), and since S100B has been shown to promote tau pathology by disrupting a substrate of GSK-3β, β-catenin, in neuronal stem cell culture (62), we hypothesized that S100B might mediate the reduction in GSK-3β activity that we observed. Indeed, we found that S100B was predominantly produced in astrocytes of 3xTg-AD mice, and was significantly reduced by anti-IL-1R-treatment (Fig. 5A, B, F). The levels of S100B showed a trend to be lower in the IgG control group, perhaps due to non-specific modulation of innate immune responses by IgG, though this difference did not reach significance. We next sought to examine the β-catenin signaling cascade in our mice. In anti-IL-1R-treated mice, the steady-state levels of β-catenin phosphorylated at Ser33/Ser37/Thr41, sites that are primarily phosphorylated by GSK-3β, showed a trend towards decrease, though failed to reach significance (Fig. 5A, C). On the other hand, we detected a significant increase of β-catenin phosphorylated at Ser552 (Fig. 5A, D). This particular phosphorylation event is mediated by Akt, and results in the nuclear translocation of β-catenin and transcriptional upregulation of pro-survival genes. Consistent with the increase in phosphor-Ser552-β-catenin, we observed that the active form of Akt (phospho-Akt) was significantly elevated in the brains of anti-IL-1R-treated mice (Fig. 5A, E; $p<0.05$). Collectively, we hypothesized that blocking IL-1 signaling in astrocytes attenuated their pro-inflammatory responses and S100B secretion, and these changes restored neuronal β-catenin signaling cascades and inhibited GSK-3β activity in the 3xTg-AD mice. Therefore, the pathological effects of IL-1 may be mediated not only by its direct action on neurons but also in the cross-talk with glial cells and neurons. However, additional studies would be needed to directly demonstrate a causal relationship between S100B and β-catenin signaling.

S100B-mediated activation of GSK-3β in a cell culture model

We next set out to test whether reduced IL-1β-induced S100B secretion from astrocytes mediated the activation of GSK-3β in neurons *in vitro*, as observed in our *in vivo* model. We exposed murine primary astrocytes to recombinant IL-1β and collected conditioned media after 24 hours. The astrocyte-conditioned media was then added to human neuroblastoma SH-SY5Y cells. Treatment of primary astrocytes with various concentrations of IL-1β (0.5-3 ng/ml) resulted in the increased production of S100B, which was released into the conditioned media. qRT-PCR showed a 3.2-fold elevation of S100B mRNA even at 0.5 ng/ml IL-1β treatment compared to control ($p<0.05$). Conditioned media from the IL-1β-treated primary astrocytes at all concentrations significantly reduced phospho-Akt and phospho-GSK-3β levels in SH-SY5Y cells and suppressed the translocation of β-catenin into the nuclear compartment (Suppl. Fig. 4A). The effect was not as great with IL-1β alone, as SH-SY5Y cells directly exposed to IL-1β only showed significant ($p<0.05$) reductions of cytosolic β-catenin, phospho-GSK-3β and phospho-Akt at the highest concentration (3 ng/ml), while no clear changes in nuclear β-catenin was detected (Suppl. Fig. 4B). We therefore used the lowest concentration of IL-1β (0.5 ng/ml) that exerted an effect on SH-SY5Y through primary astrocytes in subsequent experiments to hone in on the astrocyte-mediated pathological mechanisms of IL-1β on neuronal cells. Co-treatment of the IL-1R blocking antibody (0.1 μg/ml) with recombinant IL-1β (0.5 ng/ml) in primary astrocytes significantly reduced S100B levels (Fig. 6A) and restored β-catenin nuclear translocation in SH-SY5Y cells, along with increases in phospho-GSK-3β and phospho-Akt (Fig. 6B). Lastly, SH-SY5Y cells were treated with purified S100B protein to confirm the effect of S100B on GSK-3β and β-catenin signaling. Following 24 hr incubation, the highest concentration of S100B (5 μM) significantly reduced total β-catenin levels, and S100B activated GSK-3β in SH-SY5Y cells in a concentration-dependent manner (Fig. 6C). These data corroborate our *in vivo* findings that IL-1β modulates S100B production and secretion by astrocytes, and affects β-catenin signaling cascades in neurons.

Discussion

A chronic administration of anti-IL-1R blocking antibody in aged 3xTg-AD mice resulted in a marked change in brain inflammation, a significant attenuation of tau pathology, and reversal of cognitive deficits. Although our data on central vs. peripheral mechanisms of action are still suggestive, a fraction of systemically administered antibody appeared to cross BBB and bound IL-1 receptors on the surface of astrocytes, microglia, neurons and blood vessels in the brain. The presence of background staining or non-specific bands in all brains made the case difficult confirm or determine the exact amount of the peripherally injected antibody in the brain as well as its localization in specific cell types, yet the increased fluorescent signals in astrocytes, microglia and neurons suggest the antibody binding to the IL-1 receptor on the cell surface. Therefore, the beneficial disease-modifying effects observed in this study, including a reduction of NF-kB activation, increased levels of phagocytic markers in microglia, a suppression of S100B secretion by astrocytes, and subsequent restoration of Wnt/β-catenin signaling cascades in neurons, may in part be mediated through a direct inhibition of IL-1 signaling on these cells. However, it is important to point out that the overall suppression of neuroinflammation in the brain directly

or indirectly by the inhibition of IL-1 receptors may also exhibit beneficial disease-modifying effects in these mice. Furthermore, the peripheral effects of anti-IL-1R blocking antibody on immune cells, such as T cells, B cells and macrophages, and their impacts on CNS and AD pathologies remain to be elucidated. To support the central effect of systemically administered antibodies, a number of studies has reported penetration of peripherally-administered antibodies or endogenous antibodies generated by vaccinations into brain tissues to exhibit therapeutic effects (44, 46-52, 63, 64). Although more detailed analyses are required to confirm the direct effect of the antibody in the central nervous system, the primary aim of our study was to explore the pathological role of IL-1 signaling in AD neuropathology, and it is apparent that IL-1β plays a central role in modulating and propagating pro-inflammatory responses in the brain.

The effect of blocking IL-1β signaling on Aβ plaque pathology was unexpectedly minimal although certain Aβ species appeared to be reduced by the treatment with the IL-1R blocking antibody. Recent studies, however, reported an Aβ plaque clearance effect of pro-inflammatory cytokines, including IL-1β, through phagocytic activation of microglia in mouse models of AD (34, 35, 65, 66). Various factors, such as age and strain of mice, and transgene expression, could be involved in showing these dual effects of IL-1β in the Aβ plaque pathology, and more detailed mechanistic studies under defined conditions need to be conducted to fully understand these differential actions of microglia. For example, aging itself triggers differential activation in microglia isolated from APP/PS1 transgenic mouse model (54, 67). These studies show that aged microglia are more easily activated towards pro-inflammatory/classical activation. In our study, we used relatively old (15 months old) 3xTg-AD mice whereas studies showing that pro-inflammatory cytokines ameliorate Aβ plaques were conducted in much younger mice. This aging discrepancy may partly explain the dichotomous effects of pro-inflammatory responses in the brain and subsequent diverse pathological changes.

The inflammation- or IL-1β-induced pathological tau development has been well documented, and our findings are consistent with previous studies (25, 31-33, 53, 68). The inhibition of IL-1 signaling significantly suppressed the activation of cdk5/p25, GSK-3β and p38-MAPK, all major kinases that phosphorylate tau in neurons. A recent study demonstrated a direct effect of IL-1β secreted by microglia on neurons and subsequent activation of p38-MAPK and accumulation of tau phosphorylation (53). We believe that the observed reduction of phospho-p38-MAPK in the anti-IL-1R-treated mice may be mediated by the blockade of IL-1 receptors on neurons as well as microglia and astrocytes, or even peripheral inflammatory cells, resulting in decreased levels of IL-1β in the brain and decreased direct IL-1β signaling. On the other hand, the interplay between IL-1β and GSK-3β or cdk5 has not been well characterized. Our study examined one possible underlying mechanism by which IL-1 signaling regulates neuronal GSK-3β activation via cross-talk with astrocytes mediated by S100B.

The upregulation of S100B by IL-1β has been previously reported both *in vitro* and *in vivo* (59, 60). A number of studies suggest pathological involvement of S100B in AD and related disorders (11, 61, 69-73). In animal studies, S100B production is significantly elevated in a mouse model of AD as early as 2 months (74). Overexpression of S100B in Tg2576 mice

accelerates Aβ deposits (75). S100B also mediates the expression of Dickopff-1, which, in turn, activates GSK-3β and promotes β-catenin degradation (62). Disruption of Wnt/β-catenin pathway has been implicated in neurodevelopment as well as in neurological disorders, including AD, schizophrenia, and autism (76, 77). In AD patients, β-catenin levels are significantly reduced, and GSK-3β is upregulated and accumulates in neurons (78, 79). Glial progenitor cells from AD patients exhibit abnormal β-catenin phosphorylation and increased GSK-3β, along with impaired neurogenesis (80). In addition, in a mouse model, neuronal GSK-3β overexpression correlates with reduced nuclear β-catenin levels and increased tau hyperphosphorylation in the hippocampus (81). Collectively, these findings support our current observations in the 3xTg-AD mice and provide a possibility that one of the pathological mechanisms mediated by dysregulated pro-inflammatory responses in the brain could be the disruption of neuronal β-catenin signaling and promoting tau pathology.

In conclusion, our study elucidates one of the possible pathological pathways involved in IL-1 signaling and chronic neuroinflammation in AD. Although additional studies are required to further understand the role of neuroinflammation and neurodegeneration, the present study examined one of important pathological roles of IL-1β and neuroinflammation and provided evidence of their involvement in the pathogenesis of AD. Moreover, to our knowledge, this study is the first description that pharmacological inhibition of IL-1β signaling in an AD mouse model can abrogate AD-relevant pathology, thereby raising the possibility that targeting IL-1β signaling may result in disease-modifying therapies for AD.

Supplementary Material

Refer to Web version on PubMed Central for supplementary material.

Acknowledgments

Aβ peptides and antibodies were provided by the UCI Alzheimer's Disease Research Center (ADRC) funded by NIH/NIA grant P50AG16573 and the Institute for Memory Impairments and Neurological Disorders (UCI MIND).

This study was supported by grants from the National Institutes of Health (NIH): NIA R01AG20335 (F.M.L.), AG020241 (D.H.C.), NINDS NS050895 (D.H.C.), NIH Program Project Grant, AG00538 (F.M.L. & D.H.C.), NIH/NIAMS K99AR054695 (M.K.), and Alzheimer's Association Grant IIRG 91822 (D.H.C.).

References

1. Glass CK, Saijo K, Winner B, Marchetto MC, Gage FH. Mechanisms underlying inflammation in neurodegeneration. Cell. 2010; 140:918–934. [PubMed: 20303880]
2. Landreth GE, Reed-Geaghan EG. Toll-like receptors in Alzheimer's disease. Current topics in microbiology and immunology. 2009; 336:137–153. [PubMed: 19688332]
3. Lee YJ, Han SB, Nam SY, Oh KW, Hong JT. Inflammation and Alzheimer's disease. Archives of pharmacal research. 2010; 33:1539–1556. [PubMed: 21052932]
4. McGeer PL, Schulzer M, McGeer EG. Arthritis and anti-inflammatory agents as possible protective factors for Alzheimer's disease: a review of 17 epidemiologic studies. Neurology. 1996; 47:425–432. [PubMed: 8757015]
5. Breitner JC, Gau BA, Welsh KA, Plassman BL, McDonald WM, Helms MJ, Anthony JC. Inverse association of anti-inflammatory treatments and Alzheimer's disease: initial results of a co-twin control study. Neurology. 1994; 44:227–232. [PubMed: 8309563]

6. in t' Veld BA, Ruitenberg A, Hofman A, Launer LJ, van Duijn CM, Stijnen T, Breteler MM, Stricker BH. Nonsteroidal antiinflammatory drugs and the risk of Alzheimer's disease. The New England journal of medicine. 2001; 345:1515–1521. [PubMed: 11794217]
7. Szekely CA, Green RC, Breitner JC, Ostbye T, Beiser AS, Corrada MM, Dodge HH, Ganguli M, Kawas CH, Kuller LH, Psaty BM, Resnick SM, Wolf PA, Zonderman AB, Welsh-Bohmer KA, Zandi PP. No advantage of A beta 42-lowering NSAIDs for prevention of Alzheimer dementia in six pooled cohort studies. Neurology. 2008; 70:2291–2298. [PubMed: 18509093]
8. Bauer J, Strauss S, Schreiter-Gasser U, Ganter U, Schlegel P, Witt I, Yolk B, Berger M. Interleukin-6 and alpha-2-macroglobulin indicate an acute-phase state in Alzheimer's disease cortices. FEBS letters. 1991; 285:111–114. [PubMed: 1712317]
9. Forlenza OV, Diniz BS, Talib LL, Mendonca VA, Ojopi EB, Gattaz WF, Teixeira AL. Increased serum IL-1beta level in Alzheimer's disease and mild cognitive impairment. Dementia and geriatric cognitive disorders. 2009; 28:507–512. [PubMed: 19996595]
10. Galimberti D, Fenoglio C, Lovati C, Venturelli E, Guidi I, Corra B, Scalabrini D, Clerici F, Mariani C, Bresolin N, Scarpini E. Serum MCP-1 levels are increased in mild cognitive impairment and mild Alzheimer's disease. Neurobiology of aging. 2006; 27:1763–1768. [PubMed: 16307829]
11. Griffin WS, Stanley LC, Ling C, White L, MacLeod V, Perrot LJ, White CL 3rd, Araoz C. Brain interleukin 1 and S-100 immunoreactivity are elevated in Down syndrome and Alzheimer disease. Proceedings of the National Academy of Sciences of the United States of America. 1989; 86:7611–7615. [PubMed: 2529544]
12. Licastro F, Pedrini S, Caputo L, Annoni G, Davis LJ, Ferri C, Casadei V, Grimaldi LM. Increased plasma levels of interleukin-1, interleukin-6 and alpha-1-antichymotrypsin in patients with Alzheimer's disease: peripheral inflammation or signals from the brain? Journal of neuroimmunology. 2000; 103:97–102. [PubMed: 10674995]
13. Rota E, Bellone G, Rocca P, Bergamasco B, Emanuelli G, Ferrero P. Increased intrathecal TGF-beta1, but not IL-12, IFN-gamma and IL-10 levels in Alzheimer's disease patients. Neurol Sci. 2006; 27:33–39. [PubMed: 16688597]
14. Blum-Degen D, Muller T, Kuhn W, Gerlach M, Przuntek H, Riederer P. Interleukin-1 beta and interleukin-6 are elevated in the cerebrospinal fluid of Alzheimer's and de novo Parkinson's disease patients. Neuroscience letters. 1995; 202:17–20. [PubMed: 8787820]
15. Cacabelos RM, Barquero M, Garcia P, Alvarez XA, Varela de Seijas E. Cerebrospinal fluid interleukin-1 beta (IL-1 beta) in Alzheimer's disease and neurological disorders. Methods and findings in experimental and clinical pharmacology. 1991; 13:455–458. [PubMed: 1784142]
16. Parachikova A, Agadjanyan MG, Cribbs DH, Blurton-Jones M, Perreau V, Rogers J, Beach TG, Cotman CW. Inflammatory changes parallel the early stages of Alzheimer disease. Neurobiology of aging. 2007; 28:1821–1833. [PubMed: 17052803]
17. Weeraratna AT, Kalehua A, Deleon I, Bertak D, Maher G, Wade MS, Lustig A, Becker KG, Wood W 3rd, Walker DG, Beach TG, Taub DD. Alterations in immunological and neurological gene expression patterns in Alzheimer's disease tissues. Experimental cell research. 2007; 313:450–461. [PubMed: 17188679]
18. Bertram L, Lill CM, Tanzi RE. The genetics of Alzheimer disease: back to the future. Neuron. 2010; 68:270–281. [PubMed: 20955934]
19. Bertram L, McQueen MB, Mullin K, Blacker D, Tanzi RE. Systematic meta-analyses of Alzheimer disease genetic association studies: the AlzGene database. Nature genetics. 2007; 39:17–23. [PubMed: 17192785]
20. Harold D, Abraham R, Hollingworth P, Sims R, Gerrish A, Hamshere ML, Pahwa JS, Moskvina V, Dowzell K, Williams A, Jones N, Thomas C, Stretton A, Morgan AR, Lovestone S, Powell J, Proitsi P, Lupton MK, Brayne C, Rubinsztein DC, Gill M, Lawlor B, Lynch A, Morgan K, Brown KS, Passmore PA, Craig D, McGuinness B, Todd S, Holmes C, Mann D, Smith AD, Love S, Kehoe PG, Hardy J, Mead S, Fox N, Rossor M, Collinge J, Maier W, Jessen F, Schurmann B, van den Bussche H, Heuser I, Kornhuber J, Wiltfang J, Dichgans M, Frolich L, Hampel H, Hull M, Rujescu D, Goate AM, Kauwe JS, Cruchaga C, Nowotny P, Morris JC, Mayo K, Sleegers K, Bettens K, Engelborghs S, De Deyn PP, Van Broeckhoven C, Livingston G, Bass NJ, Gurling H, McQuillin A, Gwilliam R, Deloukas P, Al-Chalabi A, Shaw CE, Tsolaki M, Singleton AB,

Guerreiro R, Muhleisen TW, Nothen MM, Moebus S, Jockel KH, Klopp N, Wichmann HE, Carrasquillo MM, Pankratz VS, Younkin SG, Holmans PA, O'Donovan M, Owen MJ, Williams J. Genome-wide association study identifies variants at CLU and PICALM associated with Alzheimer's disease. Nature genetics. 2009; 41:1088–1093. [PubMed: 19734902]

21. Hollingworth P, Harold D, Sims R, Gerrish A, Lambert JC, Carrasquillo MM, Abraham R, Hamshere ML, Pahwa JS, Moskvina V, Dowzell K, Jones N, Stretton A, Thomas C, Richards A, Ivanov D, Widdowson C, Chapman J, Lovestone S, Powell J, Proitsi P, Lupton MK, Brayne C, Rubinsztein DC, Gill M, Lawlor B, Lynch A, Brown KS, Passmore PA, Craig D, McGuinness B, Todd S, Holmes C, Mann D, Smith AD, Beaumont H, Warden D, Wilcock G, Love S, Kehoe PG, Hooper NM, Vardy ER, Hardy J, Mead S, Fox NC, Rossor M, Collinge J, Maier W, Jessen F, Ruther E, Schurmann B, Heun R, Kolsch H, van den Bussche H, Heuser I, Kornhuber J, Wiltfang J, Dichgans M, Frolich L, Hampel H, Gallacher J, Hull M, Rujescu D, Giegling I, Goate AM, Kauwe JS, Cruchaga C, Nowotny P, Morris JC, Mayo K, Sleegers K, Bettens K, Engelborghs S, De Deyn PP, Van Broeckhoven C, Livingston G, Bass NJ, Gurling H, McQuillin A, Gwilliam R, Deloukas P, Al-Chalabi A, Shaw CE, Tsolaki M, Singleton AB, Guerreiro R, Muhleisen TW, Nothen MM, Moebus S, Jockel KH, Klopp N, Wichmann HE, Pankratz VS, Sando SB, Aasly JO, Barcikowska M, Wszolek ZK, Dickson DW, Graff-Radford NR, Petersen RC, van Duijn CM, Breteler MM, Ikram MA, Destefano AL, Fitzpatrick AL, Lopez O, Launer LJ, Seshadri S, Berr C, Campion D, Epelbaum J, Dartigues JF, Tzourio C, Alperovitch A, Lathrop M, Feulner TM, Friedrich P, Riehle C, Krawczak M, Schreiber S, Mayhaus M, Nicolhaus S, Wagenpfeil S, Steinberg S, Stefansson H, Stefansson K, Snaedal J, Bjornsson S, Jonsson PV, Chouraki V, Genier-Boley B, Hiltunen M, Soininen H, Combarros O, Zelenika D, Delepine M, Bullido MJ, Pasquier F, Mateo I, Frank-Garcia A, Porcellini E, Hanon O, Coto E, Alvarez V, Bosco P, Siciliano G, Mancuso M, Panza F, Solfrizzi V, Nacmias B, Sorbi S, Bossu P, Piccardi P, Arosio B, Annoni G, Seripa D, Pilotto A, Scarpini E, Galimberti D, Brice A, Hannequin D, Licastro F, Jones L, Holmans PA, Jonsson T, Riemenschneider M, Morgan K, Younkin SG, Owen MJ, O'Donovan M, Amouyel P, Williams J. Common variants at ABCA7, MS4A6A/MS4A4E, EPHA1, CD33 and CD2AP are associated with Alzheimer's disease. Nature genetics. 2011; 43:429–435. [PubMed: 21460840]

22. Lambert JC, Heath S, Even G, Campion D, Sleegers K, Hiltunen M, Combarros O, Zelenika D, Bullido MJ, Tavernier B, Letenneur L, Bettens K, Berr C, Pasquier F, Fievet N, Barberger-Gateau P, Engelborghs S, De Deyn P, Mateo I, Franck A, Helisalmi S, Porcellini E, Hanon O, de Pancorbo MM, Lendon C, Dufouil C, Jaillard C, Leveillard T, Alvarez V, Bosco P, Mancuso M, Panza F, Nacmias B, Bossu P, Piccardi P, Annoni G, Seripa D, Galimberti D, Hannequin D, Licastro F, Soininen H, Ritchie K, Blanche H, Dartigues JF, Tzourio C, Gut I, Van Broeckhoven C, Alperovitch A, Lathrop M, Amouyel P. Genome-wide association study identifies variants at CLU and CR1 associated with Alzheimer's disease. Nature genetics. 2009; 41:1094–1099. [PubMed: 19734903]

23. Naj AC, Jun G, Beecham GW, Wang LS, Vardarajan BN, Buros J, Gallins PJ, Buxbaum JD, Jarvik GP, Crane PK, Larson EB, Bird TD, Boeve BF, Graff-Radford NR, De Jager PL, Evans D, Schneider JA, Carrasquillo MM, Ertekin-Taner N, Younkin SG, Cruchaga C, Kauwe JS, Nowotny P, Kramer P, Hardy J, Huentelman MJ, Myers AJ, Barmada MM, Demirci FY, Baldwin CT, Green RC, Rogaeva E, George-Hyslop PS, Arnold SE, Barber R, Beach T, Bigio EH, Bowen JD, Boxer A, Burke JR, Cairns NJ, Carlson CS, Carney RM, Carroll SL, Chui HC, Clark DG, Corneveaux J, Cotman CW, Cummings JL, Decarli C, Dekosky ST, Diaz-Arrastia R, Dick M, Dickson DW, Ellis WG, Faber KM, Fallon KB, Farlow MR, Ferris S, Frosch MP, Galasko DR, Ganguli M, Gearing M, Geschwind DH, Ghetti B, Gilbert JR, Gilman S, Giordani B, Glass JD, Growdon JH, Hamilton RL, Harrell LE, Head E, Honig LS, Hulette CM, Hyman BT, Jicha GA, Jin LW, Johnson N, Karlawish J, Karydas A, Kaye JA, Kim R, Koo EH, Kowall NW, Lah JJ, Levey AI, Lieberman AP, Lopez OL, Mack WJ, Marson DC, Martiniuk F, Mash DC, Masliah E, McCormick WC, McCurry SM, McDavid AN, McKee AC, Mesulam M, Miller BL, Miller CA, Miller JW, Parisi JE, Perl DP, Peskind E, Petersen RC, Poon WW, Quinn JF, Rajbhandary RA, Raskind M, Reisberg B, Ringman JM, Roberson ED, Rosenberg RN, Sano M, Schneider LS, Seeley W, Shelanski ML, Slifer MA, Smith CD, Sonnen JA, Spina S, Stern RA, Tanzi RE, Trojanowski JQ, Troncoso JC, Van Deerlin VM, Vinters HV, Vonsattel JP, Weintraub S, Welsh-Bohmer KA, Williamson J, Woltjer RL, Cantwell LB, Dombroski BA, Beekly D, Lunetta KL, Martin ER, Kamboh MI, Saykin AJ, Reiman EM, Bennett DA, Morris JC, Montine TJ, Goate AM,

Blacker D, Tsuang DW, Hakonarson H, Kukull WA, Foroud TM, Haines JL, Mayeux R, Pericak-Vance MA, Farrer LA, Schellenberg GD. Common variants at MS4A4/MS4A6E, CD2AP, CD33 and EPHA1 are associated with late-onset Alzheimer's disease. Nature genetics. 2011; 43:436–441. [PubMed: 21460841]

24. Seshadri S, Fitzpatrick AL, Ikram MA, DeStefano AL, Gudnason V, Boada M, Bis JC, Smith AV, Carassquillo MM, Lambert JC, Harold D, Schrijvers EM, Ramirez-Lorca R, Debette S, Longstreth WT Jr, Janssens AC, Pankratz VS, Dartigues JF, Hollingworth P, Aspelund T, Hernandez I, Beiser A, Kuller LH, Koudstaal PJ, Dickson DW, Tzourio C, Abraham R, Antunez C, Du Y, Rotter JI, Aulchenko YS, Harris TB, Petersen RC, Berr C, Owen MJ, Lopez-Arrieta J, Varadarajan BN, Becker JT, Rivadeneira F, Nalls MA, Graff-Radford NR, Campion D, Auerbach S, Rice K, Hofman A, Jonsson PV, Schmidt H, Lathrop M, Mosley TH, Au R, Psaty BM, Uitterlinden AG, Farrer LA, Lumley T, Ruiz A, Williams J, Amouyel P, Younkin SG, Wolf PA, Launer LJ, Lopez OL, van Duijn CM, Breteler MM. Genome-wide analysis of genetic loci associated with Alzheimer disease. Jama. 2010; 303:1832–1840. [PubMed: 20460622]

25. Yoshiyama Y, Higuchi M, Zhang B, Huang SM, Iwata N, Saido TC, Maeda J, Suhara T, Trojanowski JQ, Lee VM. Synapse loss and microglial activation precede tangles in a P301S tauopathy mouse model. Neuron. 2007; 53:337–351. [PubMed: 17270732]

26. Giuliani F, Vernay A, Leuba G, Schenk F. Decreased behavioral impairments in an Alzheimer mice model by interfering with TNF-alpha metabolism. Brain research bulletin. 2009; 80:302–308. [PubMed: 19622386]

27. McAlpine FE, Lee JK, Harms AS, Ruhn KA, Blurton-Jones M, Hong J, Das P, Golde TE, LaFerla FM, Oddo S, Blesch A, Tansey MG. Inhibition of soluble TNF signaling in a mouse model of Alzheimer's disease prevents pre-plaque amyloid-associated neuropathology. Neurobiology of disease. 2009; 34:163–177. [PubMed: 19320056]

28. Tobinick EL, Gross H. Rapid cognitive improvement in Alzheimer's disease following perispinal etanercept administration. Journal of neuroinflammation. 2008; 5:2. [PubMed: 18184433]

29. Forloni G, Demicheli F, Giorgi S, Bendotti C, Angeretti N. Expression of amyloid precursor protein mRNAs in endothelial, neuronal and glial cells: modulation by interleukin-1. Brain Res Mol Brain Res. 1992; 16:128–134. [PubMed: 1334190]

30. Yang Y, Quitschke WW, Brewer GJ. Upregulation of amyloid precursor protein gene promoter in rat primary hippocampal neurons by phorbol ester, IL-1 and retinoic acid, but not by reactive oxygen species. Brain Res Mol Brain Res. 1998; 60:40–49. [PubMed: 9748493]

31. Li Y, Liu L, Barger SW, Griffin WS. Interleukin-1 mediates pathological effects of microglia on tau phosphorylation and on synaptophysin synthesis in cortical neurons through a p38-MAPK pathway. J Neurosci. 2003; 23:1605–1611. [PubMed: 12629164]

32. Kitazawa M, Oddo S, Yamasaki TR, Green KN, LaFerla FM. Lipopolysaccharide-induced inflammation exacerbates tau pathology by a cyclin-dependent kinase 5-mediated pathway in a transgenic model of Alzheimer's disease. J Neurosci. 2005; 25:8843–8853. [PubMed: 16192374]

33. Sheng JG, Zhu SG, Jones RA, Griffin WS, Mrak RE. Interleukin-1 promotes expression and phosphorylation of neurofilament and tau proteins in vivo. Experimental neurology. 2000; 163:388–391. [PubMed: 10833312]

34. Shaftel SS, Kyrkanides S, Olschowka JA, Miller JN, Johnson RE, O'Banion MK. Sustained hippocampal IL-1 beta overexpression mediates chronic neuroinflammation and ameliorates Alzheimer plaque pathology. The Journal of clinical investigation. 2007; 117:1595–1604. [PubMed: 17549256]

35. Tachida Y, Nakagawa K, Saito T, Saido TC, Honda T, Saito Y, Murayama S, Endo T, Sakaguchi G, Kato A, Kitazume S, Hashimoto Y. Interleukin-1 beta up-regulates TACE to enhance alpha-cleavage of APP in neurons: resulting decrease in Abeta production. Journal of neurochemistry. 2008; 104:1387–1393. [PubMed: 18021299]

36. Blurton-Jones M, Kitazawa M, Martinez-Coria H, Castello NA, Muller FJ, Loring JF, Yamasaki TR, Poon WW, Green KN, LaFerla FM. Neural stem cells improve cognition via BDNF in a transgenic model of Alzheimer disease. Proceedings of the National Academy of Sciences of the United States of America. 2009; 106:13594–13599. [PubMed: 19633196]

37. Martinez-Coria H, Green KN, Billings LM, Kitazawa M, Albrecht M, Rammes G, Parsons CG, Gupta S, Banerjee P, LaFerla FM. Memantine improves cognition and reduces Alzheimer's-like neuropathology in transgenic mice. Am J Pathol. 2010; 176:870–880. [PubMed: 20042680]
38. Cribbs DH, Ghochikyan A, Vasilevko V, Tran M, Petrushina I, Sadzikava N, Babikyan D, Kesslak P, Kieber-Emmons T, Cotman CW, Agadjanyan MG. Adjuvant-dependent modulation of Th1 and Th2 responses to immunization with beta-amyloid. International immunology. 2003; 15:505–514. [PubMed: 12663680]
39. Head E, Pop V, Vasilevko V, Hill M, Saing T, Sarsoza F, Nistor M, Christie LA, Milton S, Glabe C, Barrett E, Cribbs D. A two-year study with fibrillar beta-amyloid (Abeta) immunization in aged canines: effects on cognitive function and brain Abeta. J Neurosci. 2008; 28:3555–3566. [PubMed: 18385314]
40. Kitazawa M, Trinh DN, LaFerla FM. Inflammation induces tau pathology in inclusion body myositis model via glycogen synthase kinase-3beta. Annals of neurology. 2008; 64:15–24. [PubMed: 18318434]
41. Goedert M, Jakes R, Vanmechelen E. Monoclonal antibody AT8 recognises tau protein phosphorylated at both serine 202 and threonine 205. Neuroscience letters. 1995; 189:167–169. [PubMed: 7624036]
42. Tsoporis JN, Marks A, Van Eldik LJ, O'Hanlon D, Parker TG. Regulation of the S100B gene by alpha 1-adrenergic stimulation in cardiac myocytes. American journal of physiology. 2003; 284:H193–203. [PubMed: 12388300]
43. Langmann T, Mauerer R, Schmitz G. Human ATP-binding cassette transporter TaqMan low-density array: analysis of macrophage differentiation and foam cell formation. Clinical chemistry. 2006; 52:310–313. [PubMed: 16449213]
44. Tan J, Town T, Crawford F, Mori T, DelleDonne A, Crescentini R, Obregon D, Flavell RA, Mullan MJ. Role of CD40 ligand in amyloidosis in transgenic Alzheimer's mice. Nature neuroscience. 2002; 5:1288–1293.
45. Wong ML, Licinio J. Localization of interleukin 1 type I receptor mRNA in rat brain. Neuroimmunomodulation. 1994; 1:110–115. [PubMed: 7489320]
46. Dodart JC, Bales KR, Gannon KS, Greene SJ, DeMattos RB, Mathis C, DeLong CA, Wu S, Wu X, Holtzman DM, Paul SM. Immunization reverses memory deficits without reducing brain Abeta burden in Alzheimer's disease model. Nature neuroscience. 2002; 5:452–457.
47. Hartman RE, Izumi Y, Bales KR, Paul SM, Wozniak DF, Holtzman DM. Treatment with an amyloid-beta antibody ameliorates plaque load, learning deficits, and hippocampal long-term potentiation in a mouse model of Alzheimer's disease. J Neurosci. 2005; 25:6213–6220. [PubMed: 15987951]
48. Kotilinek LA, Bacskai B, Westerman M, Kawarabayashi T, Younkin L, Hyman BT, Younkin S, Ashe KH. Reversible memory loss in a mouse transgenic model of Alzheimer's disease. J Neurosci. 2002; 22:6331–6335. [PubMed: 12151510]
49. Lee EB, Leng LZ, Zhang B, Kwong L, Trojanowski JQ, Abel T, Lee VM. Targeting amyloid-beta peptide (Abeta) oligomers by passive immunization with a conformation-selective monoclonal antibody improves learning and memory in Abeta precursor protein (APP) transgenic mice. The Journal of biological chemistry. 2006; 281:4292–4299. [PubMed: 16361260]
50. Oddo S, Vasilevko V, Caccamo A, Kitazawa M, Cribbs DH, LaFerla FM. Reduction of soluble Abeta and tau, but not soluble Abeta alone, ameliorates cognitive decline in transgenic mice with plaques and tangles. The Journal of biological chemistry. 2006; 281:39413–39423. [PubMed: 17056594]
51. Wang A, Das P, Switzer RC 3rd, Golde TE, Jankowsky JL. Robust amyloid clearance in a mouse model of Alzheimer's disease provides novel insights into the mechanism of amyloid-beta immunotherapy. J Neurosci. 2011; 31:4124–4136. [PubMed: 21411653]
52. Wilcock DM, Rojiani A, Rosenthal A, Levkowitz G, Subbarao S, Alamed J, Wilson D, Wilson N, Freeman MJ, Gordon MN, Morgan D. Passive amyloid immunotherapy clears amyloid and transiently activates microglia in a transgenic mouse model of amyloid deposition. J Neurosci. 2004; 24:6144–6151. [PubMed: 15240806]

53. Bhaskar K, Konerth M, Kokiko-Cochran ON, Cardona A, Ransohoff RM, Lamb BT. Regulation of tau pathology by the microglial fractalkine receptor. Neuron. 2010; 68:19–31. [PubMed: 20920788]
54. Jimenez S, Baglietto-Vargas D, Caballero C, Moreno-Gonzalez I, Torres M, Sanchez-Varo R, Ruano D, Vizuete M, Gutierrez A, Vitorica J. Inflammatory response in the hippocampus of PS1M146L/APP751SL mouse model of Alzheimer's disease: age-dependent switch in the microglial phenotype from alternative to classic. J Neurosci. 2008; 28:11650–11661. [PubMed: 18987201]
55. Sheng JG, Jones RA, Zhou XQ, McGinness JM, Van Eldik LJ, Mrak RE, Griffin WS. Interleukin-1 promotion of MAPK-p38 overexpression in experimental animals and in Alzheimer's disease: potential significance for tau protein phosphorylation. Neurochemistry international. 2001; 39:341–348. [PubMed: 11578769]
56. Basu A, Krady JK, O'Malley M, Styren SD, DeKosky ST, Levison SW. The type 1 interleukin-1 receptor is essential for the efficient activation of microglia and the induction of multiple proinflammatory mediators in response to brain injury. J Neurosci. 2002; 22:6071–6082. [PubMed: 12122068]
57. Kim SH, Smith CJ, Van Eldik LJ. Importance of MAPK pathways for microglial pro-inflammatory cytokine IL-1 beta production. Neurobiology of aging. 2004; 25:431–439. [PubMed: 15013563]
58. Lee SC, Liu W, Dickson DW, Brosnan CF, Berman JW. Cytokine production by human fetal microglia and astrocytes. Differential induction by lipopolysaccharide and IL-1 beta. J Immunol. 1993; 150:2659–2667. [PubMed: 8454848]
59. de Souza DF, Leite MC, Quincozes-Santos A, Nardin P, Tortorelli LS, Rigo MM, Gottfried C, Leal RB, Goncalves CA. S100B secretion is stimulated by IL-1beta in glial cultures and hippocampal slices of rats: Likely involvement of MAPK pathway. Journal of neuroimmunology. 2009; 206:52–57. [PubMed: 19042033]
60. Sheng JG, Ito K, Skinner RD, Mrak RE, Rovnaghi CR, Van Eldik LJ, Griffin WS. In vivo and in vitro evidence supporting a role for the inflammatory cytokine interleukin-1 as a driving force in Alzheimer pathogenesis. Neurobiology of aging. 1996; 17:761–766. [PubMed: 8892349]
61. Peskind ER, Griffin WS, Akama KT, Raskind MA, Van Eldik LJ. Cerebrospinal fluid S100B is elevated in the earlier stages of Alzheimer's disease. Neurochemistry international. 2001; 39:409–413. [PubMed: 11578776]
62. Esposito G, Scuderi C, Lu J, Savani C, De Filippis D, Iuvone T, Steardo L Jr, Sheen V, Steardo L. S100B induces tau protein hyperphosphorylation via Dickopff-1 up-regulation and disrupts the Wnt pathway in human neural stem cells. Journal of cellular and molecular medicine. 2008; 12:914–927. [PubMed: 18494933]
63. Masliah E, Rockenstein E, Adame A, Alford M, Crews L, Hashimoto M, Seubert P, Lee M, Goldstein J, Chilcote T, Games D, Schenk D. Effects of alpha-synuclein immunization in a mouse model of Parkinson's disease. Neuron. 2005; 46:857–868. [PubMed: 15953415]
64. Levites Y, Das P, Price RW, Rochette MJ, Kostura LA, McGowan EM, Murphy MP, Golde TE. Anti-Abeta42- and anti-Abeta40-specific mAbs attenuate amyloid deposition in an Alzheimer disease mouse model. The Journal of clinical investigation. 2006; 116:193–201. [PubMed: 16341263]
65. Chakrabarty P, Ceballos-Diaz C, Beccard A, Janus C, Dickson D, Golde TE, Das P. IFN-gamma promotes complement expression and attenuates amyloid plaque deposition in amyloid beta precursor protein transgenic mice. J Immunol. 2010; 184:5333–5343. [PubMed: 20368278]
66. Chakrabarty P, Jansen-West K, Beccard A, Ceballos-Diaz C, Levites Y, Verbeeck C, Zubair AC, Dickson D, Golde TE, Das P. Massive gliosis induced by interleukin-6 suppresses Abeta deposition in vivo: evidence against inflammation as a driving force for amyloid deposition. Faseb J. 2010; 24:548–559. [PubMed: 19825975]
67. Hickman SE, Allison EK, El Khoury J. Microglial dysfunction and defective beta-amyloid clearance pathways in aging Alzheimer's disease mice. J Neurosci. 2008; 28:8354–8360. [PubMed: 18701698]
68. Tanji K, Mori F, Imaizumi T, Yoshida H, Satoh K, Wakabayashi K. Interleukin-1 induces tau phosphorylation and morphological changes in cultured human astrocytes. Neuroreport. 2003; 14:413–417. [PubMed: 12634494]

69. Hu J, Castets F, Guevara JL, Van Eldik LJ. S100 beta stimulates inducible nitric oxide synthase activity and mRNA levels in rat cortical astrocytes. The Journal of biological chemistry. 1996; 271:2543–2547. [PubMed: 8576219]
70. Li Y, Barger SW, Liu L, Mrak RE, Griffin WS. S100beta induction of the proinflammatory cytokine interleukin-6 in neurons. Journal of neurochemistry. 2000; 74:143–150. [PubMed: 10617115]
71. Li Y, Wang J, Sheng JG, Liu L, Barger SW, Jones RA, Van Eldik LJ, Mrak RE, Griffin WS. S100 beta increases levels of beta-amyloid precursor protein and its encoding mRNA in rat neuronal cultures. Journal of neurochemistry. 1998; 71:1421–1428. [PubMed: 9751173]
72. Liu L, Li Y, Van Eldik LJ, Griffin WS, Barger SW. S100B-induced microglial and neuronal IL-1 expression is mediated by cell type-specific transcription factors. Journal of neurochemistry. 2005; 92:546–553. [PubMed: 15659225]
73. Petzold A, Jenkins R, Watt HC, Green AJ, Thompson EJ, Keir G, Fox NC, Rossor MN. Cerebrospinal fluid S100B correlates with brain atrophy in Alzheimer's disease. Neuroscience letters. 2003; 336:167–170. [PubMed: 12505619]
74. Sheng JG, Mrak RE, Bales KR, Cordell B, Paul SM, Jones RA, Woodward S, Zhou XQ, McGinness JM, Griffin WS. Overexpression of the neuritotrophic cytokine S100beta precedes the appearance of neuritic beta-amyloid plaques in APPV717F mice. Journal of neurochemistry. 2000; 74:295–301. [PubMed: 10617132]
75. Mori T, Koyama N, Arendash GW, Horikoshi-Sakuraba Y, Tan J, Town T. Overexpression of human S100B exacerbates cerebral amyloidosis and gliosis in the Tg2576 mouse model of Alzheimer's disease. Glia. 2010; 58:300–314. [PubMed: 19705461]
76. De Ferrari GV, Moon RT. The ups and downs of Wnt signaling in prevalent neurological disorders. Oncogene. 2006; 25:7545–7553. [PubMed: 17143299]
77. Kozlovsky N, Belmaker RH, Agam G. GSK-3 and the neurodevelopmental hypothesis of schizophrenia. Eur Neuropsychopharmacol. 2002; 12:13–25. [PubMed: 11788236]
78. Pei JJ, Braak E, Braak H, Grundke-Iqbal I, Iqbal K, Winblad B, Cowburn RF. Distribution of active glycogen synthase kinase 3beta (GSK-3beta) in brains staged for Alzheimer disease neurofibrillary changes. Journal of neuropathology and experimental neurology. 1999; 58:1010–1019. [PubMed: 10499443]
79. Zhang Z, Hartmann H, Do VM, Abramowski D, Sturchler-Pierrat C, Staufenbiel M, Sommer B, van de Wetering M, Clevers H, Saftig P, De Strooper B, He X, Yankner BA. Destabilization of beta-catenin by mutations in presenilin-1 potentiates neuronal apoptosis. Nature. 1998; 395:698–702. [PubMed: 9790190]
80. He P, Shen Y. Interruption of beta-catenin signaling reduces neurogenesis in Alzheimer's disease. J Neurosci. 2009; 29:6545–6557. [PubMed: 19458225]
81. Lucas JJ, Hernandez F, Gomez-Ramos P, Moran MA, Hen R, Avila J. Decreased nuclear beta-catenin, tau hyperphosphorylation and neurodegeneration in GSK-3beta conditional transgenic mice. The EMBO journal. 2001; 20:27–39. [PubMed: 11226152]

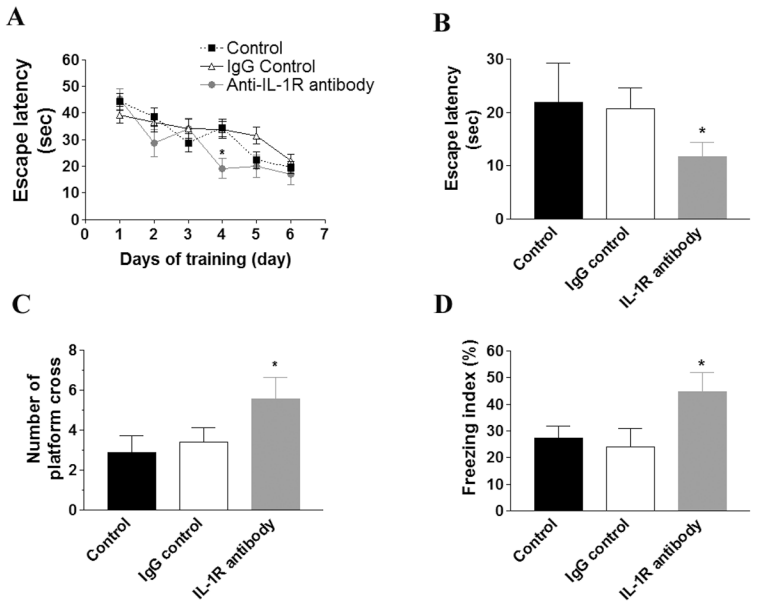

Figure 1. Administering an IL-1R blocking antibody rescues hippocampus-dependent cognitive impairments in the 3xTg-AD mice

(A) Acquisition curve during training of MWM is expressed as mean ± S.E.M. No significant difference was observed among the groups. (B) Escape latency and (C) number of crosses on platform location for 24-hr retention trial in MWM. Each bar is expressed as mean ± S.E.M., and *p<0.05 compared to control and IgG control groups. (D) The freezing index of CFC is expressed as mean ± S.E.M. *p<0.05 compared to control and IgG control groups. The number of mice tested: n=10 for control and IgG control, and n=8 for IL-1R blocking antibody treatment.

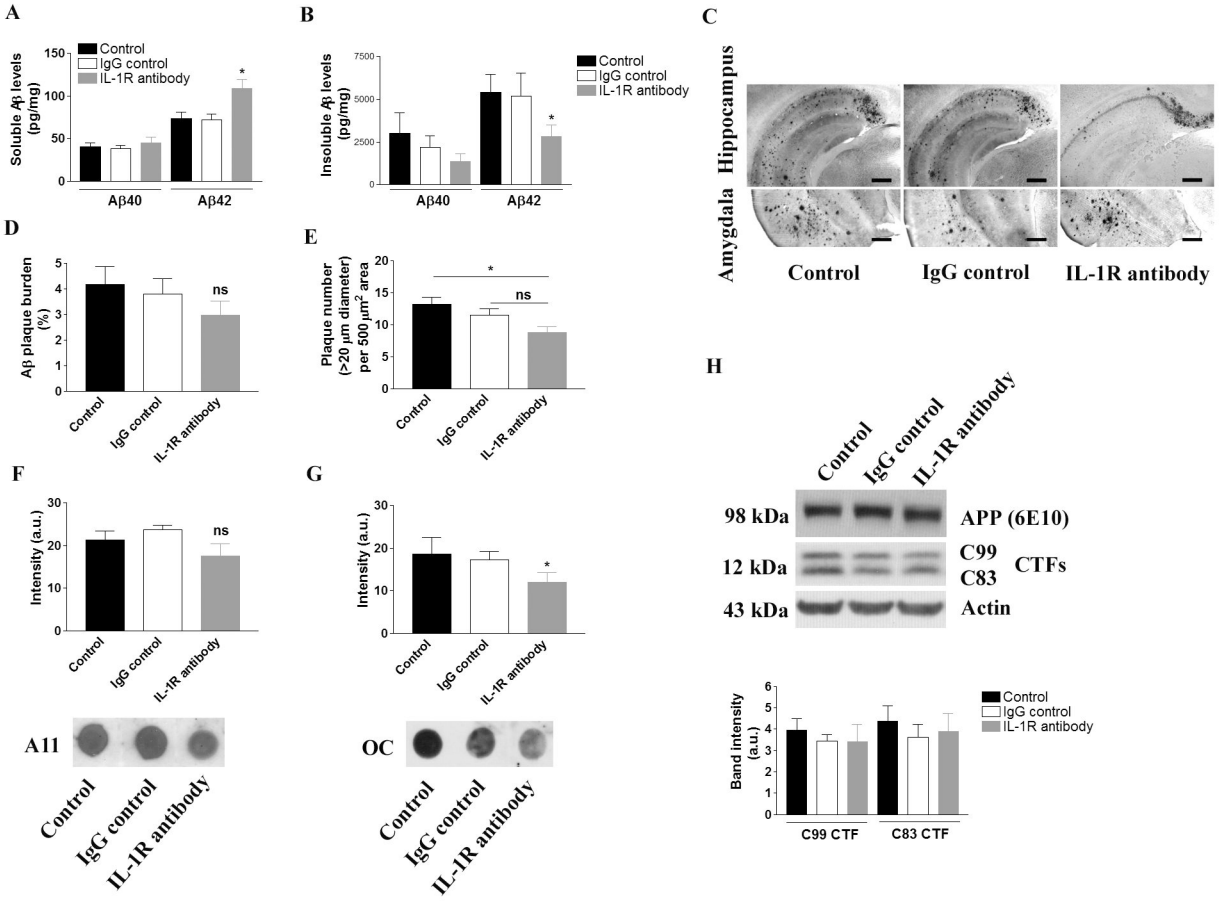

Figure 2. Blocking IL-1 signaling and effect on amyloid pathology in the 3xTg-AD mice

(A) Quantitative Aβ ELISA in detergent-soluble brain fraction and (B) detergent-insoluble (formic acid soluble) brain fraction. Each bar is expressed as mean ± S.E.M., and *p<0.05 compared to control and IgG control groups. (C) Representative immunohistochemical staining of amyloid plaque burden in the hippcampus and amygdala. Anti-$A\beta_{42}$ specific antibody detects aggregated Aβ-containing plaques (scale bar = 500 μm). (D) Amyloid burden in the hippocampus, sebiculum, entorhinal cortex and amygdala is expressed as a bar graph. ns stands for not significant. (E) Plaque count (over 20 μm in diameter) in 500 μm^2 subfield in the hippocampus, subiculum, entorhinal cortex and amygdala is expressed in the bar graph (mean ± S.E.M.). *p<0.05 compared to control, and ns stands for not significant. (F) Dot blot analysis of oligomeric Aβ species using antibody A11, and (G) antibody OC. Each bar is expressed as mean ± S.E.M., and *p<0.05 compared to control and IgG control groups. More dot blot data for A11 and OC are found in Suppl. Fig. 2B. (H) Immunoblot analysis of APP processing in the brain following the treatment. The densitometric analysis of C99 and C83 fragments was shown in the graph. Each bar is expressed as mean ± S.E.M. No statistical significance was obtained. The number of mice tested: n=10 for control and IgG control, and n=8 for IL-1R blocking antibody treatment.

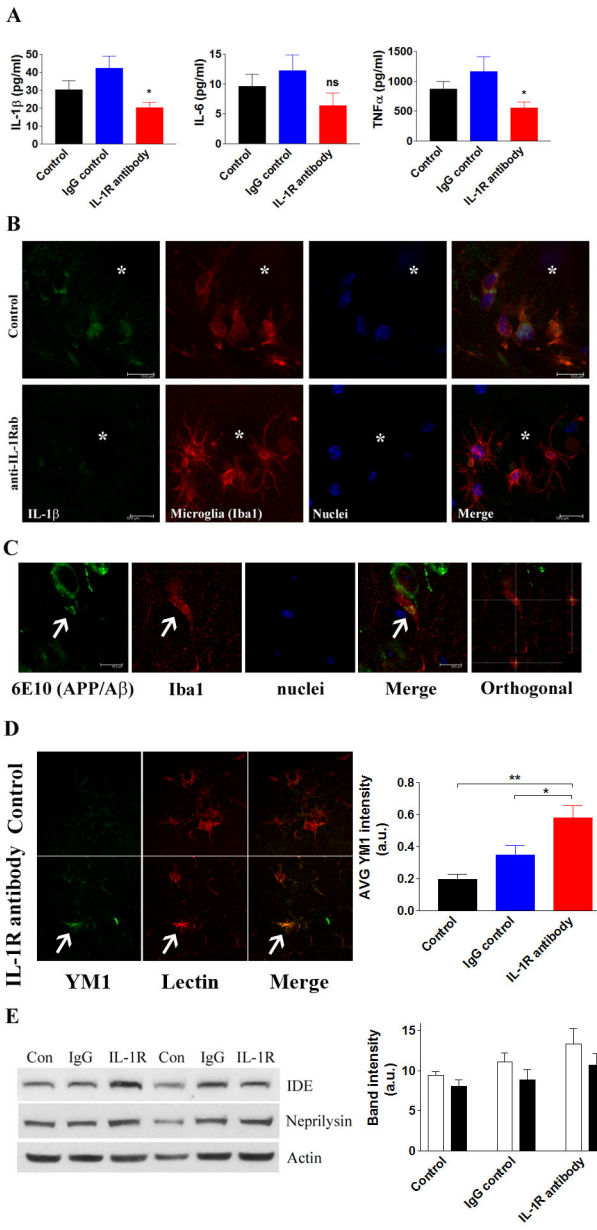

Figure 3. Blocking IL-1 signaling decreases pro-inflammatory cytokines and enhances microglial phagocytosis

(A) ELISA analysis of selected pro-inflammatory cytokines. Each bar is expressed as mean ± S.E.M. (n=10 for control and IgG control, and n=8 for anti-IL-1R treatment), and *p<0.05 compared to control and IgG control groups. (B) IL-1β levels are decreased in animals receiving the anti-IL-1R blocking antibody. Double immunofluorescent staining with IL-1β and microglia. Asterisks indicate amyloid plaques (scale bar = 10 μm). (C) Suppressing IL-1 signaling promotes the phagocytosis of Aβ by microglia. Representative double-immunofluorescent staining with Aβ (6E10) and microglia (Iba1) in the brain of anti-IL-1R-treated 3xTg-AD mice. Arrows indicate Aβ within microglial compartment (scale bar = 10 μm). (D) Double immunofluorescent staining of YM1 (green) and tomato lectin (red) around

Aβ plaques in control and anti-IL-1R antibody-treated mice. Arrow indicates activated microglia with high YM1 expression. YM1 fluorescent intensity was measured and plotted in graph (mean ± S.E.M.). *$p<0.05$ or **$p<0.01$ compared to IgG control or control, respectively. (E) Immunoblots and densitometric analyses of Aβ degrading enzymes, insulin degrading enzyme (IDE) and neprilysin in the brain homogenates (n=10 for control and IgG control, n=8 for IL-1R blocking antibody treatment). No statistical significance is detected by densitometric analyses (mean ± S.E.M.).

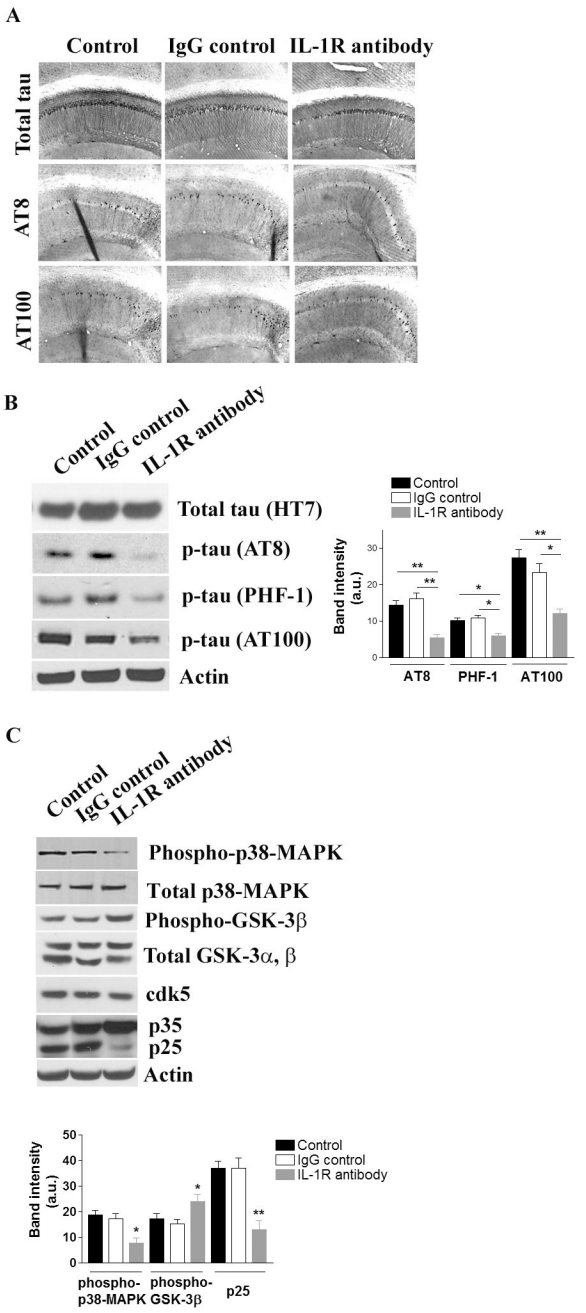

Figure 4. Suppressing IL-1 signaling attenuates tau pathology in the 3xTg-AD mice

(A) Tau pathology is attenuated by blocking IL-1 signaling. Representative immunohostochemical staining with various tau antibodies; HT7 – total tau, AT8 – phosphorylated tau at Ser 199 and Ser 202, and AT100 – phosphorylated tau at Ser 212 and Thr 214. (B) Immunoblot and densitometric analyses of changes in the steady-state levels of phosphorylated tau in the brain. Each bar is expressed as mean ± S.E.M. (n=10 for control and IgG control, and n=8 for anti-IL-1R treatment), and *p<0.05 or **p<0.01 compared to control and IgG control groups. More immunoblot data for phospho-tau are found in Suppl. Fig. 2D. (C) Suppressing IL-1 signaling results in decreased activations of tau kinases.

Immunoblot and densitometric analyses of the steady-state levels of GSK-3β, cdk5/p35/p25 and p38-MAPK. Each bar is expressed as mean ± S.E.M. (n = 10 for control and IgG control, and n=8 for anti-IL-1R treatment), and *p<0.05 or **p<0.01 compared to control and IgG control groups.

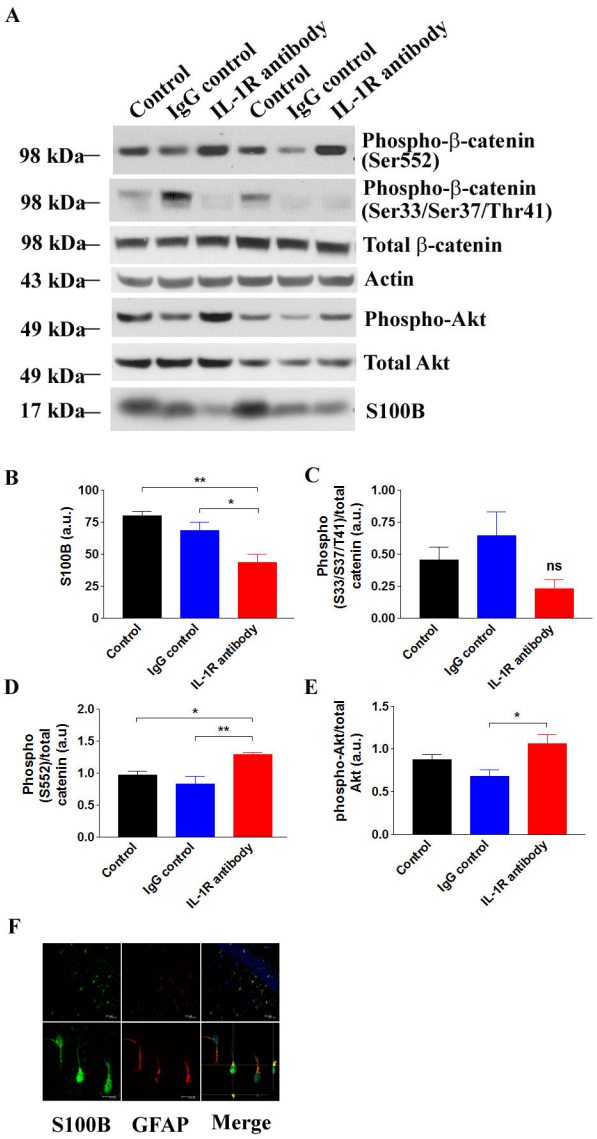

Figure 5. S100B and β-catenin signaling are altered in anti-IL-1R antibody-treated 3xTg-AD mice

(A) Immunoblot analysis of the steady-state levels of phospho-β-catenin at Ser 33/Ser 37/Thr 41. (B-E) Densitometric analysis of the intensity of immunoblots. Each bar is expressed as mean ± S.E.M. (n=6 for all groups), and *p<0.05 or **p<0.01 compared to corresponding group or ns for non-significant. (F) Double immunostaining with S100B (green) and GFAP (astrocyte marker, red) confirms that S100B is predominantly produced in astrocytes in the brain of 3xTg-AD mice. TOTO-3 (blue) is used to counter-stain nuclei. Scale bars - 20 μm (upper panels) and 10 μm (lower panels).

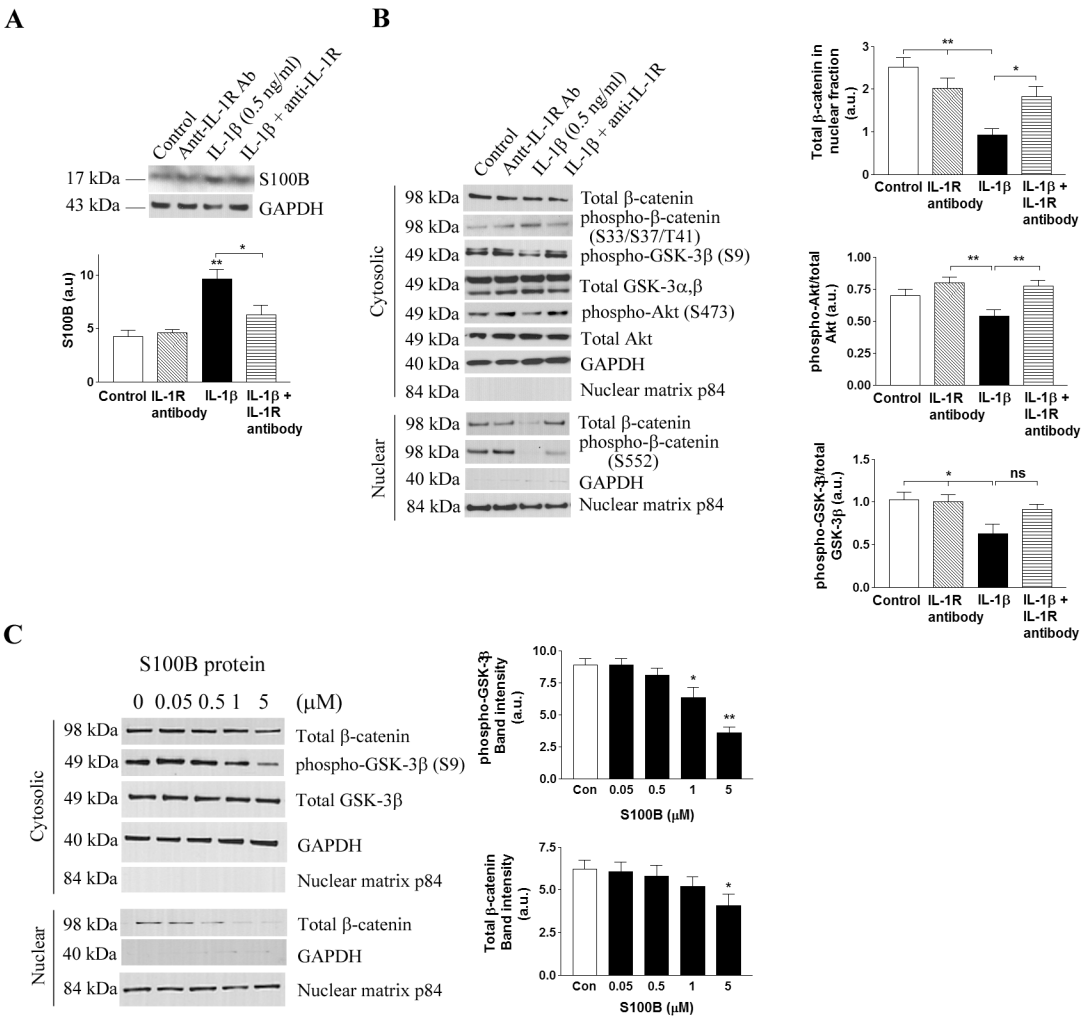

Figure 6. IL-1β triggers S100B-mediated alterations in β-catenin signaling in neurons

(A) Immunoblot and densitometric analysis (mean ± S.E.M.) of S100B in primary astrocytes exposed to recombinant IL-1β with or without anti-IL-1R blocking antibody for 24 hrs. *p<0.05 or **p<0.01 compared to control (n=6). GAPDH is used for a loading control. (B) Conditioned media from mouse primary astrocytes exposed to 0.5 ng/ml mouse recombinant IL-1β with or without 0.1 μg/ml anti-IL-1R blocking antibody for 24 hrs are used to treat SH-SY5Y cells for 24 hrs, and subseqent changes in β-catenin signaling cascades are detected by immunoblots. Densitometric analyses (mean ± S.E.M.) show a significant changes in nuclear translocation of β-catenin, cytosolic phospho-GSK-3β (at Ser 9) and phospho-Akt (at Ser 473) in co-treatment with anti-IL-1R blocking antibody (*p<0.05 or **p<0.01, n=6). GAPDH and nuclear matrix p84 are used to confirm no cross contamination between cytosolic and nuclear fractions, respectively. (C) SH-SY5Y cells are treated with various doses of purified S100B protein for 24 hrs, and changes in β-catenin and GSK-3β are examined by immunoblot analysis. Densitometric analysis of band intensity (mean ± S.E.M.) is expressed in a bar graph, and *p<0.05 or **p<0.01 compared to control (two separate experiments, n=4 per experiment).